

Charge-Density Waves in Self-Assembled Halogen-Bridged Metal Chains

K. Swamy, A. Menzel, R. Beer, and E. Bertel*

Institute of Physical Chemistry, University of Innsbruck, A-6020 Innsbruck, Austria

(Received 24 August 2000)

Self-assembled growth of an ordered layer of Pt-Br-Pt chains on a Pt(110) surface is demonstrated. Upon slight doping with excess bromine, charge-density wave (CDW) domains separated by well-localized solitons are observed in the Br/Pt layer by scanning tunneling microscopy. Depending on annealing and adatom concentration, a global, long-range-ordered CDW ground state can be established. Angle-resolved UV photoemission data reveal the corresponding Fermi surface and its removal upon the Peierls transition. The CDW phase is stable to well above room temperature.

DOI: 10.1103/PhysRevLett.86.1299

PACS numbers: 71.45.Lr, 63.20.Kr, 68.37.Ef, 79.60.Dp

Low-dimensional electronic systems exhibit peculiar properties not normally found in three-dimensional (3D) metals. Electron-electron, electron-phonon, and spin-phonon interactions are strongly enhanced [1]. The resulting many-body effects in (quasi-) 1D systems give rise to critical phenomena, in particular, symmetry breaking phase transitions [2].

The strong electron-phonon coupling is related to the tendency of quasi-1D systems to exhibit extended parallel sections of the Fermi surface separated by a constant wave vector $|\mathbf{q}| = 2k_F$ (Fermi surface nesting) [3,4]. This allows a zero-energy, finite-momentum electron excitation with considerable oscillator strength. Consequently, at sufficiently low temperature the polarization function $\chi(\mathbf{q})$ diverges, which in turn causes a phonon softening (Kohn anomaly) in the acoustic phonon branch or even a static lattice distortion, when the phonon frequency $\omega(\mathbf{q})$ drops to zero. Such a distortion is associated with a charge-density modulation and is called a charge-density wave (CDW) [5]. The periodicity is determined by the wave vector \mathbf{q} and thus depends on the details of the Fermi surface. If the Fermi surface can be modified, for instance, by deposition of appropriately chosen adatoms, one may be able to vary the CDW periodicity and hence the surface geometry.

A few years ago, Carpinelli *et al.* [6] proposed this approach in order to switch between different surface structures. In our paper we tested the feasibility of this proposal. First, we show that self-structuring of an adsorption system on a suitable metallic template yields a quasi-1D surface compound. Second, by doping this system with adsorbates we transfer it into a CDW ground state. In contrast to CDW systems studied thus far, different CDW phases (for instance, with or without long-range order, respectively) can be obtained simply by choosing suitable doping conditions. The phase transition into the CDW ground state can be directly observed by scanning tunneling microscopy (STM). Low-energy electron diffraction (LEED) is used to determine atomic periodicities and the temperature stability, and angle-resolved UV photoemission (ARUPS) to explore Fermi surface properties.

In our search for a suitable low-dimensional system we were guided by the well-known tendency of halogen-

bridged platinum linear-chain compounds to develop a CDW ground state [1,7–9]. By using the strongly anisotropic Pt(110) surface [10] as a template and by carefully depositing bromine, we were able to obtain an ordered surface array of linear Pt-Br structures. Bromine was dosed onto the surface by means of a solid state electrolysis cell. During Br exposures, the pressure remained in the low 10^{-11} mbar range. Coverages were determined by temperature programmed desorption spectroscopy calibrated against LEED patterns (medium-coverage range) and STM images (low-coverage range). The Br-covered surface was then cautiously annealed to successively higher temperatures and the resulting structures were examined by LEED and room-temperature STM (Raster-scope 3000, Danish Micro Engineering). A detailed account of Br adsorption at various temperatures is given elsewhere [11]. Up to a temperature of about 400 K, adsorbed Br atoms were found in pairs on the surface. At $T > 400$ K the pairs become unstable and the Br atoms are substitutionally incorporated into next-nearest-neighbor positions within the densely packed Pt atom rows. At sufficiently high coverage [$\Theta_{\text{Br}} \approx 0.5$ ML (monolayers) ($1 \text{ ML} = 9.2 \times 10^{18} \text{ m}^{-2}$)], extended Pt-Br-Pt chains are formed in this way. The chains arrange themselves in regular patterns, either with the Pt atoms coordinated to the Br atoms in the neighboring chains ($\begin{smallmatrix} \text{Pt-Br-Pt-Br} \\ \text{Br-Pt-Br-Pt} \end{smallmatrix}$), giving rise to a local $c(2 \times 2)$ unit cell, or with Pt atoms coordinated in Pt atoms, i.e., ($\begin{smallmatrix} \text{Pt-Br-Pt-Br} \\ \text{Pt-Br-Pt-Br} \end{smallmatrix}$), forming a local $p(2 \times 1)$ unit cell. At a coverage of precisely 0.5 ML, and after annealing to ~ 750 K, the former arrangement proves to be slightly favored and an almost perfectly ordered $c(2 \times 2)$ -Br/Pt(110) overlayer is formed [Fig. 1(a)].

While not obvious at first sight, the quasi-1D character of this overlayer is indicated by two experimental observations: (1) Desorption of only a few percent of the Br causes a strongly 1D disordered missing/added row structure to appear. Entire segments of Pt-Br-Pt chains are expelled from the $c(2 \times 2)$ layer, leaving behind missing rows. The expelled material partially reassembles into Pt-Br-Pt chains on top of the $c(2 \times 2)$ layer upon cooling down (added rows), as seen in Fig. 1(b). (ii) In our ARUPS measurements some of the electronic bands (particularly

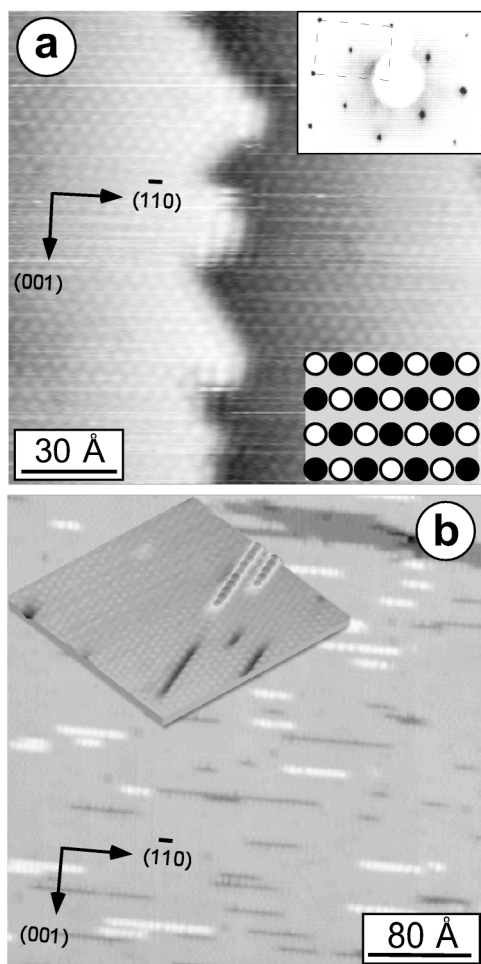


FIG. 1. Bromine adsorption on Pt(110). (a) STM image ($U_{\text{bias}} = 54$ mV) of the $c(2 \times 2)$ -Br/Pt(110) structure formed after deposition of 0.5 monolayers of Br on Pt(110) and subsequent annealing to ~ 750 K. Upper right inset: the corresponding LEED pattern. Lower right inset: ball model of the structure (black balls, Br atoms; white balls, Pt atoms). (b) The same overlayer after desorption of a few percent of Br atoms ($U_{\text{bias}} = 9$ mV). A one-dimensionally disordered missing-row/added-row structure is formed. The added rows consist of Pt-Br-Pt chains, which are also the building blocks of the perfect $c(2 \times 2)$ structure. Inset: 3D view of the missing-row/added-row structure.

those around the Fermi level) show much stronger dispersion in the $(1\bar{1}0)$ direction parallel to the Pt-Br-Pt chains than in the (001) direction perpendicular to the chains, indicating an extremely anisotropic electron mobility.

Drawing on the analogy between our Pt-Br-Pt chains and the halogen-bridged transition-metal linear-chain molecules, where the ground state depends significantly on the presence of various counterions, we proceeded to explore the influence of surface dopants. A natural choice was to use bromine as an acceptor species. An extremely small Br coverage (< 0.005 ML) deposited at $T = 300$ K onto the $c(2 \times 2)$ overlayer causes a spectacular change of the STM image (Fig. 2). The excess Br atoms sit in pairs [12] on top of the $c(2 \times 2)$ layer, as will be seen below. They are imaged as depressions, which is a well-known

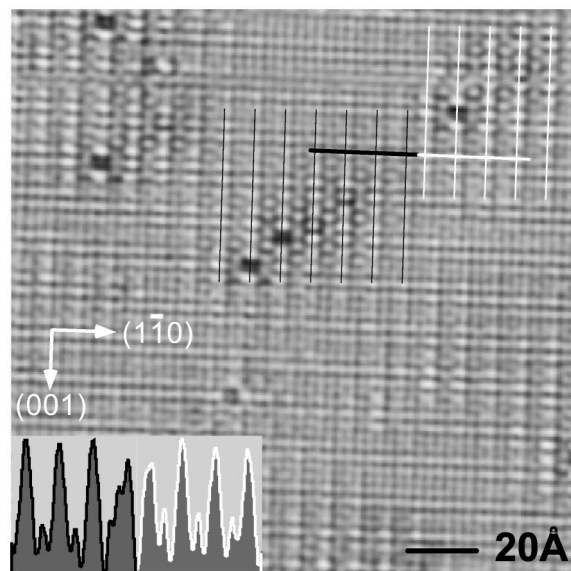


FIG. 2. Charge-density wave phase without long-range order. STM image ($U_{\text{bias}} = -330$ mV) of the $c(2 \times 2)$ -Br/Pt(110) layer after doping with 0.003 ML Br_2 . The doping molecules (imaged as holes) are surrounded by local (3×1) CDW domains. Inset: line profile obtained from a scan along the black and white line (corrugation 0.32 Å) connecting two CDW domains, which are out of phase. The phase discommensuration, or soliton, can be clearly discerned.

effect for electronegative adsorbates [13]. Around each dopant pair domains with a (3×1) periodicity along $(1\bar{1}0)$ are formed. Simultaneously, an extreme unidirectional broadening of the centered spot in the $c(2 \times 2)$ LEED pattern indicates that the correlation between neighboring chains is lost, i.e., the chain alignment varies randomly between the two types of coordination discussed above. As shown by the STM height scan in Fig. 2, the (3×1) antiphase domains are separated from each other by phase discommensurations (solitons) [14], which are well localized (to within ~ 2 nm distances) in the direction of the rows, but less well defined perpendicular to the rows. Apart from the extreme anisotropy underlining the 1D character of the present system, the effect is qualitatively similar to the defect-mediated condensation of a CDW observed by Plummer and co-workers on Sn/Ge(111) [15,16]. In that system, too, antiphase CDW domains are separated by atomically abrupt boundaries. In the present case, however, even at 300 K the decay length of the charge-density modulation exceeds the mean distance between defects (note, for instance, that the amplitude along the height profile shown in the inset of Fig. 2 is almost constant). As in Fig. 2 the domain size is limited by the presence of the surrounding antiphase domains rather than the finite decay length; we surveyed domain sizes at extremely low coverages ($\Theta_{\text{Br}} < 0.001$ ML). The largest domain diameter we found in both the (001) and the $(1\bar{1}0)$ directions was about 90 Å, but even under these conditions the domain size seemed to be limited by neighboring antiphase domains. The large extension of (3×1) domains in real space corresponds to

a strong localization in reciprocal space. In other words, the charge-density modulation in Fig. 2 is characterized essentially by a single, well-defined wave vector \mathbf{q} . The observed (3×1) periodicity is indeed independent of the tunneling bias [see also Figs. 3(b) and 3(c)], in contrast to Friedel oscillations observed previously in two-dimensional systems [17,18]. There, the apparent wavelength of Friedel oscillations measured by STM changed with the bias (this was used to map out the corresponding surface-state dispersion [17]). The fact that the present instability is associated with a single wave vector \mathbf{q} points to a divergence in the electron response function $\chi(\mathbf{q})$ at $|\mathbf{q}| = 2k_F$, a typical trait of (quasi-) 1D systems.

In addition to the larger decay length there is another interesting difference in the disordered CDW phase described in Plummer and co-workers [15,16]: In the present case the CDW domains are always pinned with a crest of the CDW to the doping molecules. In Sn/Ge(111) the CDW domains were pinned in a similar way to the defects. However, in the present system the distribution of the pinning centers is random. Accordingly, most of the CDW domains are associated with only one pinning center, in contrast to Sn/Ge(111). For low adatom concentrations

even at room temperature no CDW-mediated hopping [15] is observed in the phase shown in Fig. 2.

If the present CDW phase is annealed to 600 K, the Br pairs break up into atoms diffusing individually on the surface. This is indicated by twice the number of holes appearing in the STM images and by a significant change in the pattern of the holes. The Br pairs are imaged as almost rectangular depressions (see Fig. 2), while the separated Br atoms appear as perfectly circular holes (Fig. 3). The latter are observed to be mobile at room temperature. As a consequence, the antiphase domains disappear in favor of one global, long-range-ordered (3×1) CDW ground state, which extends over the whole terraces. The (3×1) periodicity appears also in the LEED pattern [Fig. 3(a)]. This provides additional proof that a modulation of the atom positions is associated with the doping-induced long-range modulation of the electronic density of states imaged in the STM. This is precisely the definition of a CDW. The transition from the $c(2 \times 2)$ to the (3×1) phase is entirely reversible. Careful annealing to 780 K removes the excess Br atoms and converts the CDW phase back into a perfect $c(2 \times 2)$ overlayer. It is worth emphasizing that the transition from the $c(2 \times 2)$ into the (3×1) CDW phase is associated with a bond-length modulation of the order of at most a few tenths of an Å [8].

Interestingly, the pinning regime is different in the global CDW phase. Although the Br atoms preferably sit on the crest of the CDW, other locations are occasionally found [Fig. 3(d)]. In fact, the excess Br atoms are mobile and the time constant for hopping amounts to a few seconds at 300 K (the mobility is not induced by the STM, as checked by applying different bias and scan directions). While a strong commensurability pinning is expected for the global phase, it is surprising that the impurity pinning is so weak as to allow a hopping of the doping atoms at 300 K.

A CDW requires the existence of a Fermi surface with an appropriate nesting vector. Hence we examined the system by ARUPS (Fig. 4): In the undoped $c(2 \times 2)$ overlayer [Fig. 4(a)] a band is seen to cross the Fermi level at a wave vector $\mathbf{q}_{(1\bar{1}0)} \sim 0.70 \text{ \AA}^{-1}$. It disperses downward with increasing wave vector (holelike dispersion). This Fermi wave vector is slightly off the ideal nesting vector for a threefold periodicity, namely, 0.756 \AA^{-1} . After transition into the (3×1) phase the Fermi surface is removed, as expected for a CDW. While in the $c(2 \times 2)$ phase the band exhibits an appreciable dispersion perpendicular to the Pt-Br-Pt chains, doping reduces the dispersion substantially [Fig. 4(b)]. The doping causes a nonuniform shift of k_F towards the ideal value in such a way that the curvature of the Fermi surface is reduced, and hence the Fermi surface nesting, is improved. Thus the (3×1) CDW ground state is stabilized relative to the $c(2 \times 2)$ structure.

Because of the freshly introduced (3×1) periodicity, the band is folded back and, locally, a gap opens up. The folding back is clearly evident from Fig. 4(a). For a Br

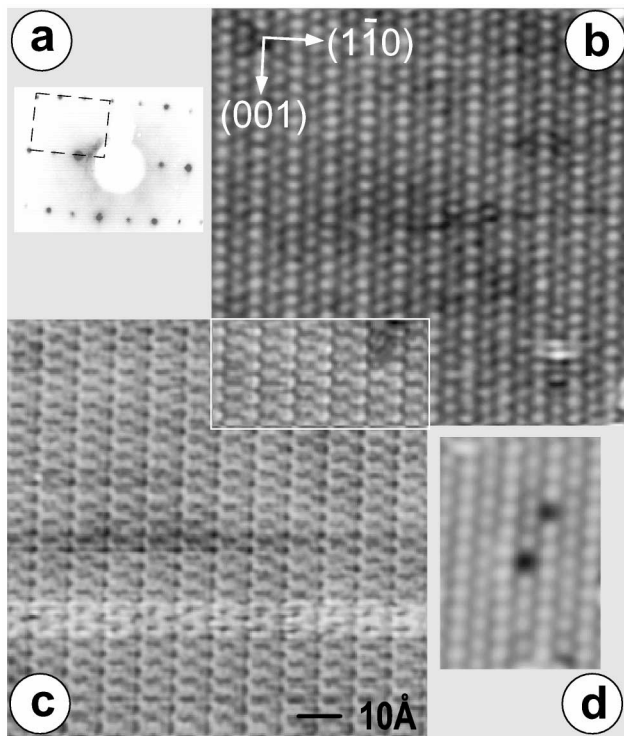


FIG. 3. Global charge density wave phase. (a) LEED pattern of the CDW phase ($\Theta_{\text{Br}} = 0.505 \text{ ML}$). Dashed rectangle: (1×1) unit cell. (b) Empty state STM image of the CDW phase recorded with a simple bias of $U_{\text{bias}} = +10 \text{ mV}$. (c) Filled state image of the same area recorded at $U_{\text{bias}} = -110 \text{ mV}$. The central inset shows the result of a numerical contrast inverse. It reproduces almost perfectly the empty state image. The $100 \times 100 \text{ \AA}^2$ image area was chosen to be free of doping atoms. (d) STM image showing two doping atoms located at different positions with respect to the phase of the underlying CDW.

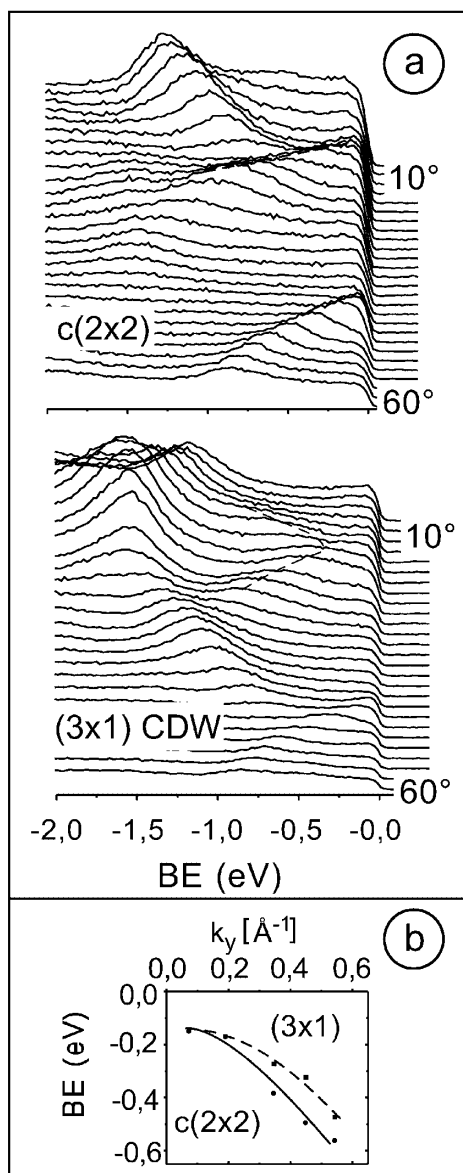


FIG. 4. Angle-resolved UV-photoemission spectra (HeI) of $c(2 \times 2)$ -Br/Pt(110) and of the (3×1) CDW phase ($T = 120$ K). (a) In the undistorted $c(2 \times 2)$ phase a band is seen to cross the Fermi level at $k_x \approx 0.70 \text{ \AA}^{-1}$ ($\sim 20^\circ$ polar angle). In the (3×1) CDW phase the band is folded back (see dashed line as a guide for the eye) and the corresponding Fermi surface is removed. (b) Dispersion of the band perpendicular to the Pt-Br-Pt chains $E(k_y)$ measured at constant $k_x = 0.75 \text{ \AA}^{-1}$.

doping concentration of about 0.5% of a ML, the temperature dependent intensity variation of the $1/3$ LEED beams was found to be qualitatively similar to that reported by Plummer and co-workers for Sn/Ge(111) [15]. In the present case also, an almost linear decrease is observed. It extrapolates to zero intensity at ~ 530 K as opposed

to ~ 270 K in Sn/Ge(111). Mean-field theory predicts a Peierls gap of the order of $\Delta = 3.53kT_P$. The remarkable stability of the CDW up to $T > 500$ K implies that here the Peierls gap is of the order of tenths of an eV [2].

In summary, both STM and ARUPS show that an extraordinarily stable CDW can be triggered by slight surface doping of the $c(2 \times 2)$ -Br/Pt(110) surface. Even at constant temperature, different CDW phases can be realized in this way, lending the system an extremely interesting playground for the exploration of CDW phase transitions, pinning behavior, soliton formation, and other phenomena associated with low dimensionality.

We thank W. Moritz for useful discussions. This work was financially supported by the Austrian Science Fund.

*Author to whom correspondence should be addressed.

- [1] A. R. Bishop, *Synth. Met.* **86**, 2203 (1997).
- [2] S. Kagoshima, H. Nagasawa, and T. Sambongi, *One-Dimensional Conductors* (Springer, Berlin, 1988).
- [3] E. Tosatti, in *Electronic Surface and Interface States in Metallic Systems*, edited by E. Bertel and M. Donath (World Scientific, Singapore, 1995), p. 67.
- [4] E. Hulpke, *Electronic Surface and Interface States in Metallic Systems* (Ref. [3]), p. 91.
- [5] G. Grüner, *Density Waves in Solids* (Addison-Wesley, Reading, MA, 1994).
- [6] J. M. Carpinelli, H. H. Weitering, E. W. Plummer, and R. Stumpf, *Nature (London)* **381**, 398 (1996).
- [7] Th. D. Ryan and R. E. Rundle, *J. Am. Chem. Soc.* **83**, 2814 (1961).
- [8] M. Alouani, J. M. Wilkins, R. C. Albers, and J. M. Wills, *Phys. Rev. Lett.* **71**, 1415 (1993).
- [9] G. S. Kanner *et al.*, *Phys. Rev. B* **50**, 18 682 (1994).
- [10] M. A. Krzyzowski *et al.*, *Phys. Rev. B* **50**, 18 505 (1994).
- [11] K. Swamy, P. Hanesch, P. Sandl, and E. Bertel, *Surf. Sci.* (to be published).
- [12] Circumstantial evidence indicates that these pairs are dissociated Br atoms in closely spaced adsorption sites (see Ref. [11]).
- [13] I. S. Tilinin, M. K. Rose, J. C. Dunphy, M. Salmeron, and M. A. Van Hove, *Surf. Sci.* **418**, 511 (1998).
- [14] P. Bak, *Rep. Prog. Phys.* **45**, 587 (1982).
- [15] H. H. Weitering, J. M. Carpinelli, A. V. Melechko, J. Zhang, M. Bartowiak, and E. W. Plummer, *Science* **285**, 2107 (1999).
- [16] A. V. Melechko, J. Braun, H. H. Weitering, and E. W. Plummer, *Phys. Rev. Lett.* **83**, 999 (1999).
- [17] M. F. Crommie, C. P. Lutz, and D. M. Eigler, *Nature (London)* **363**, 524 (1993).
- [18] Y. Hasegawa and Ph. Avouris, *Phys. Rev. Lett.* **71**, 1071 (1993).